

Review

Artifactual Lung Ultrasonography: It Is a Matter of Traps, Order, and Disorder

Gino Soldati ^{1,2,*}, Andrea Smargiassi ³ , Libertario Demi ⁴  and Riccardo Inchingolo ³

¹ Diagnostic and Interventional Ultrasound Unit, Ospedale Valle del Serchio, 55032 Castelnuovo di Garfagnana, Lucca, Italy

² Fondazione Toscana Gabriele Monasterio, 56100 Pisa, Italy

³ Pulmonary Medicine Unit, Department of Cardiovascular and Thoracic Sciences-Fondazione Policlinico Universitario “A. Gemelli” IRCCS, 00168 Rome, Italy; andrea.smargiassi@policlinicogemelli.it (A.S.); riccardo.inchingolo@policlinicogemelli.it (R.I.)

⁴ Department of Information Engineering and Computer Science, University of Trento, 38122 Trento, Italy; libertario.demi@unitn.it

* Correspondence: soldatigino@yahoo.it; Tel.: +3-934-9726-9851

Received: 15 December 2019; Accepted: 20 February 2020; Published: 25 February 2020



Featured Application: The differential diagnosis between a normally aerated lung and a lung with interstitial pathology is based on the interpretation of ultrasound vertical artifacts. However, the physical basis of these artifacts and their correlations with the causal pulmonary pathology is not known in depth. Theoretical and experimental studies strongly support the hypothesis that the link between non-consolidative parenchymal pathological conditions of the lung and the presence of vertical artifacts is mediated by the acoustic properties of the pleura and is caused by a structural change in the geometry and connectivity of subpleural air spaces. The future development of lung ultrasound needs a better knowledge of ultrasound artefactual semiotics, a valid correlations between artefactual evidence and the superficial lung structure, and, not least, the development of ultrasound equipment, software and probes, specifically dedicated to lung sonography.

Abstract: When inspecting the lung with standard ultrasound B-mode imaging, numerous artifacts can be visualized. These artifacts are useful to recognize and evaluate several pathological conditions in Emergency and Intensive Care Medicine. More recently, the interest of the Pulmonologists has turned to the echographic study of the interstitial pathology of the lung. In fact, all lung pathologies which increase the density of the tissue, and do not consolidate the organ, are characterized by the presence of ultrasound artifacts. Many studies of the past have only assessed the number of vertical artifacts (generally known as B-Lines) as a sign of disease severity. However, recent observations suggest that the appearance of the individual artifacts, their variability, and their internal structure, may play a role for a non-invasive characterization of the surface of the lungs, directing the diagnoses and identifying groups of diseases. In this review, we discuss the meaning of lung ultrasound artifacts, and introduce hypothesis on the correlation between their presence and the structural variation of the sub-pleural tissue in light of current knowledge of the acoustic properties of the pleural plane.

Keywords: lung; ultrasound; artefact; pulmonary; sonography

1. Introduction

In the last years, lung ultrasonography has gained ever-growing clinical interest and curiosity because of its peculiar ability to acquire clinical information at bedside, its non-invasiveness and

low cost. In particular settings (emergency medicine, intensive care unit) its utility has been well demonstrated [1–3]. More recently, pulmonologists and pediatricians started to use chest ultrasound for detecting pleural diseases, consolidations, bronchiolitis, interstitial lung pathology and critical pulmonary conditions of the newborn [4,5]. However, the development of lung ultrasonography for exploring non-consolidated organs, has been disordered and not supported by a strong knowledge of the physical mechanisms that underlie pulmonary artifacts. Lung ultrasonography is comparable to a standard morphological sonography only when assessing a pulmonary consolidation, a tissue without air, which is in direct contact with the visceral pleura. In this case, the clinicians evaluate anatomic images, representing the real structure of the diseased organ.

Normally, chest X ray is the first diagnostic tool for pneumonia, pulmonary contusions, lung cancer, and pulmonary infarction. The possibility to assess lung consolidations in several conditions by using ultrasound has a wide clinical impact, limiting, optimizing and justifying ionizing radiations [6–9]. On one hand, however, chest X ray has the advantage to show a panoramic view, while lung consolidations not reaching the visceral pleura can be completely missed by ultrasound [10]. On the other hand, chest ultrasonography is able to provide more information about the characteristics of consolidations reaching the visceral pleura [11,12] such as: air dynamic or static bronchogram [13], fluid bronchogram [11], parenchymal abscesses, necrotic areas, vascularization and sonographic contrast-enhancement information [14]. Pleural diseases are the other relevant target for clinical ultrasound. For pleural effusions ultrasound can be considered the main diagnostic tool, giving us the possibility to evaluate the sonographic appearance, extension, mechanical effects on work of breathing, and interventional guidance [15–17]. Neither chest X-ray nor Chest CT scan is able to provide such relevant details to clinicians.

Differently, when the lung surface is denser but not yet consolidated, the large acoustic impedance gradient between the chest wall and the pulmonary tissue containing air prevents every anatomic representation, and the scan results in the visualization of many kind of vertical artifacts generally known as B-Lines [18,19]. Little is known about the best method for evaluating vertical lung artifacts because they look different at different depths, depend on the machine/probe and on the frequency employed. Probably, many “cosmetic” regulations of modern machines influence the visualization of the artifacts. Tissue Harmonic Imaging, compound imaging, pre- and post-processing techniques and filters can modify the appearance of the artifacts [19].

When imaging the pathologic yet not fully consolidated lung surface, the basic assumptions behind standard ultrasound imaging are severely unmet. Firstly, the presence of air in the volume of interest results in strong heterogeneities in speed of sound. Consequently, performing the typical time-to-space conversion based on an average speed of sound value, as normally implemented in commercial scanners, is not appropriate in this case. Secondly, the high reflection coefficient experienced by ultrasound waves at multiple and distributed air–tissue interfaces produces a highly scattering environment, where multiple scattering phenomena are strong, and it is therefore not possible to model the echo-signals received by the probe by simply assuming a first-order scattering medium. In this context, it is impossible to link the time of arrival of the echo signals to the spatial location of the corresponding scatterers. Therefore, beyond the pleural-line, ultrasound images cannot be considered to be an anatomical representation of the lung structure.

However, when considering the typical frequency range employed for ultrasound medical imaging, say 1–10 MHz, the wavelength of the corresponding pressure waves is small enough, i.e., from 0.15 to 1.5 mm, to be able to feel even small alterations in the lung structure.

Consequently, different artifacts can be produced by the application of standard image reconstruction algorithms to these signals [20].

In this case, the target of ultrasonography is represented by several pathologies involving peripheral lung that do not determine parenchymal consolidation with focal or diffuse extension. It is the case of fibrosing interstitial lung diseases, early septal cardiogenic pulmonary edema, cardiogenic pulmonary edema with alveolar flooding, acute respiratory distress syndrome, pulmonary hemorrhage,

and focal or diffuse inflammatory abnormalities [4,5]. Generally, the main diagnostic tool for these pathologies is chest CT scan. Obviously, Chest CT scan is able to provide morphological and panoramic views of these pathologies. In these contexts, different artifacts provide different information for clinicians, which is useful to get both the correct diagnosis and to indicate the correct diagnostic process. The final goal of chest ultrasonography and artifacts analysis in these pathologies is not to substitute chest CT scan, but to become the fifth pillar of medical examination, providing signs to clinicians not obtainable by classic semiotic [8].

Finally, when lung is normally inflated, the anatomic representation, even more so, is not possible. The normal pleural-line acts essentially as a specular reflector to ultrasound waves, resulting in the visualization of reverberation artifacts of the pleural-line, and both mirror and replica effects of the chest wall are visible. This so-called “normal pattern”, when characterized by the detection of lung points and by the absence of sliding sign, is indicative of pneumothorax [20,21].

In conclusion, chest ultrasonography has the potential to help physicians facing different pathologic conditions afflicting the respiratory system, especially in case of acute onset dyspnea. The BLUE-protocol (Bedside Lung Ultrasound in Emergency) is an example, and it has been proposed as an easy and feasible approach to acute dyspnea, reaching 90.5% of accuracy and quickly providing appropriate diagnosis [22].

In this review, the acoustic properties of the normal and pathological pleural-line will be discussed together with the acoustic behavior of the sub-pleural lung when the pleural-line is not a strong near-perfect reflector.

2. Terminology

In this paper, classical terms employed by the clinicians to describe ultrasound findings in lung ultrasonography (A-Lines, B-Lines, and Interstitial Syndrome) will not be used [23]. According to recent observations addressing the origin of the ultrasound lung artifacts [24,25], we will use terms consistent with the principles that govern the ultrasound propagation through aerated and variously porous tissues. When necessary, the usual lung ultrasound lexicon will be recalled and addressed to the involved physical phenomena.

A-Lines is a generic term indicating horizontal artifacts related to a normal lung surface. In this review, we consider these artifacts as the summation of the reverberation effects, due to the pleural-line and myofascial acoustic interfaces of the chest wall, and the mirror effects (variable in its expression in relation to the thickness of the chest wall) reproducing beyond the pleural line, in a specular way, the myofascial planes of the chest wall (Figure 1).

B-Lines are defined as discrete laser-like vertical hyperechoic artifacts that arise with a narrow base from the pleural line, extending to the bottom of the screen without fading, and moving synchronously with lung sliding [1,6]. As B-lines show great heterogeneity and they look different at different levels [7], we will simply call the B-Lines “vertical artifacts” (Figure 2).

From a clinical point of view, they indicate a denser sub-pleural lung, but not yet consolidated, caused by: (1) interstitial pathology enlarging the interstitial tissue but sparing residual peripheral air spaces; (2) pathologic deflations of a normal healthy lung or pathologic subversion of peripheral air spaces; and (3) mixed situations [23,24]. The term “Interstitial Syndrome” can thus be transformed in “Hyperdense pre-consolidated sub-pleural lung”. In cognitive terms, the vertical artifacts in lung sonography represent acoustic information relative to a physical state (porosity or full/empty ratio) of a relatively thin and superficial layer of the lung.

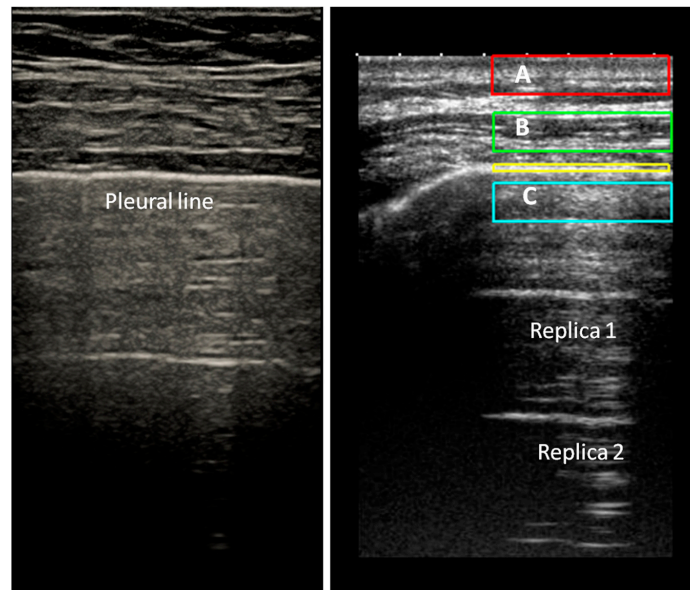


Figure 1. Normal pleural line. **(Left):** Healthy subject, B Mode image. The pleural line is regular, below the pleural line, the image does not represent the anatomy of the lung. **(Right):** Below the echogenic pleural surface the replica effects of the pleural line can be seen. In the box C, the replica of the contents of box A and the mirror effect of the contents of the box B are added together. (Images obtained with a commercially available machine, Toshiba Aplio XV, equipped with a linear probe, 9 MHz, without harmonic imaging).

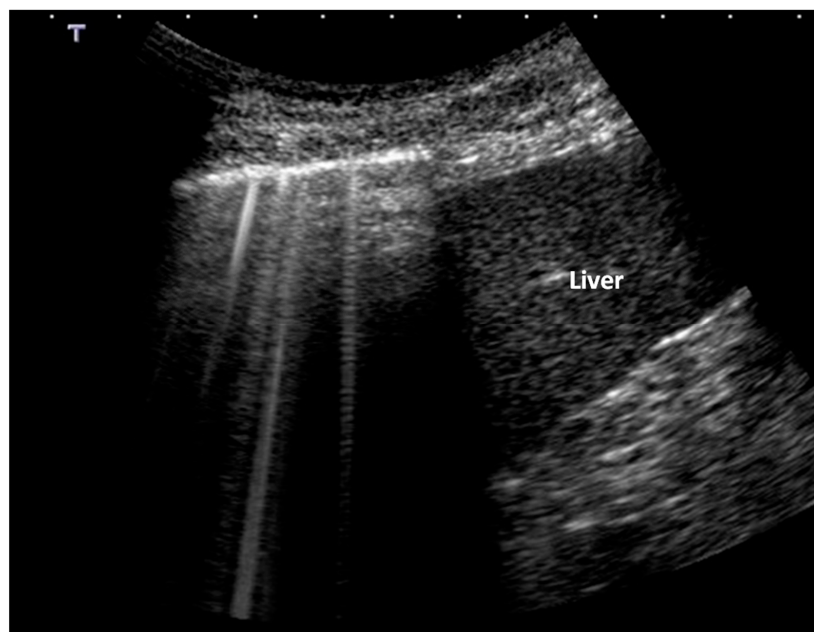


Figure 2. Vertical artifacts at the base of the right lung. Early pulmonary edema. Note the presence of a uniform white artifact along with artefact showing clear bands overlap. Early pulmonary edema. (Image obtained with a commercially available machine, Toshiba Aplio XV, equipped with a convex probe, 6 MHz, without harmonic imaging).

3. How Normal Anatomy of Pleural Plane is Represented in Ultrasound Images

The visceral pleura, firmly covering the lungs and the interlobular fissures, together with the parietal pleural layer, lining the thoracic cage and the virtual space between them, act like a single surface of discontinuity. In sonographic images the visceral and parietal pleura appear as an echogenic

regular pleural-line [26]. Pleural membranes are covered by a single layer of flattened mesothelial cells (1–4 μm thick). Underneath the mesothelial cells, there is a layer of connective tissue (10–15 μm thick). In adult lungs, the aerated lobules are placed below the visceral pleura and are separated from each other by the interlobular septa, incompletely demarcating polyhedral units of lung parenchyma.

Each lobule measures from 1 to 2.5 cm and contains three to five acini, composed by alveolar spaces [27]. Interlobular septa are made of connective tissue, pulmonary veins and lymphatics. Their thickness is no more than 100 μm and they represent the main acoustic discontinuities along the normal pleura.

Considering this kind of cortical lung porosity, the ultrasound pulse that hits a smooth visceral pleura, is reflected almost completely. Once the reflected echo has reached the probe, it can have enough energy to be partially back-reflected and reach the pleural-line again. In this case, the probe receives two echoes coming from the pleural-line. Consequently, with the transformation of the signal from the time domain to the space domain, the obtained spatial function shows two pleural-lines: the first is the real one and the second is an artifactual line, localized at a double distance (Figure 1).

This process can also generate more than two pleural-lines (replica effects) [28]. These lines, in the case of a healthy pleura, are regular, bright, and relatively thin. In literature, these horizontal artifacts are named A-Lines. We prefer to identify these artifacts, together with every sub-pleural mirror and replica effects of the chest wall tissues, as specular artifacts. In general, they indicate a healthy pleural surface [4].

4. Acoustic Behavior of the Diseased Pleura

The pleura and the lung are strictly linked and share many pathologic conditions. Inflammatory and hydrostatic edema can involve the thin layer of connective tissue underneath the mesothelial cells [29]. This tissue is continuous with the sub-pleural lung interstice. Therefore, a sub-pleural edema is highly interconnected with the underlying interstitial lung tissue. Pleural fibrosis can be the result of many inflammatory processes such as rheumatoid pleurisy, bacterial empyema, asbestos exposure, malignancy, retained hemothorax, and drugs. In all these situations, a clear separation between sub-mesothelial and superficial interstitial fibrosis is impossible [27]. The fibrotic remodeling in Idiopathic Pulmonary Fibrosis (IPF) begins in the basal sub-pleural regions and progresses toward the lung apices over time [30]. In patients with IPF, High Resolution CT (HRCT) scan morphometric analysis shows a complex and connected reticulum of fibrous tissue extending from the pleura into the underlying lung tissue (lobular fibrosis). Partially or completely scarred lobules, devoid of alveolar spaces, microcysts, honeycombing and fibroblast foci are features of IPF histopathology which determine a high disordered sub-pleural morphology [31,32].

Based on the above premises, the difference between a healthy and a diseased pleura (in the hyperdense non-consolidated range of the lung pathology) resides in the presence of regions with different acoustic characteristics along the surface of the pleural plane, normally acting as an acoustic reflector. Because of this anatomic re-configuration, and in particular because of the presence of residual air spaces, local arrangements may exist where the energy of the acoustic pulses, which are transmitted by the probe, is partially trapped (acoustic traps) (Figure 3) [13,28].

An acoustic trap is characterized by a transonic access (likely from 0.1 to 1 mm and beyond) to the sub-pleural enlarged interstitial tissue, with a variable shape and content (water, cells, and connective tissue), and that is surrounded by residual air. Such a volume is the core of the trap, since the multiple-scattering phenomena happening within the trap act as an ultrasound source and can explain the genesis of the vertical artifacts [28,33].

A diseased pleura, covering a hyperdense non-consolidated lung, shows a variable number of irregularities and acoustic traps on its surface which are able to break its physiological acoustic reflectivity, thus generating and opening a variety of paths (channels) through which ultrasound can be captured. Finally, it is worth noting that when we speak of a distribution of structures with variable

morphology and acoustic properties along a diseased pleura, we implicitly introduce a concept of relative order or disorder of these structures [31].

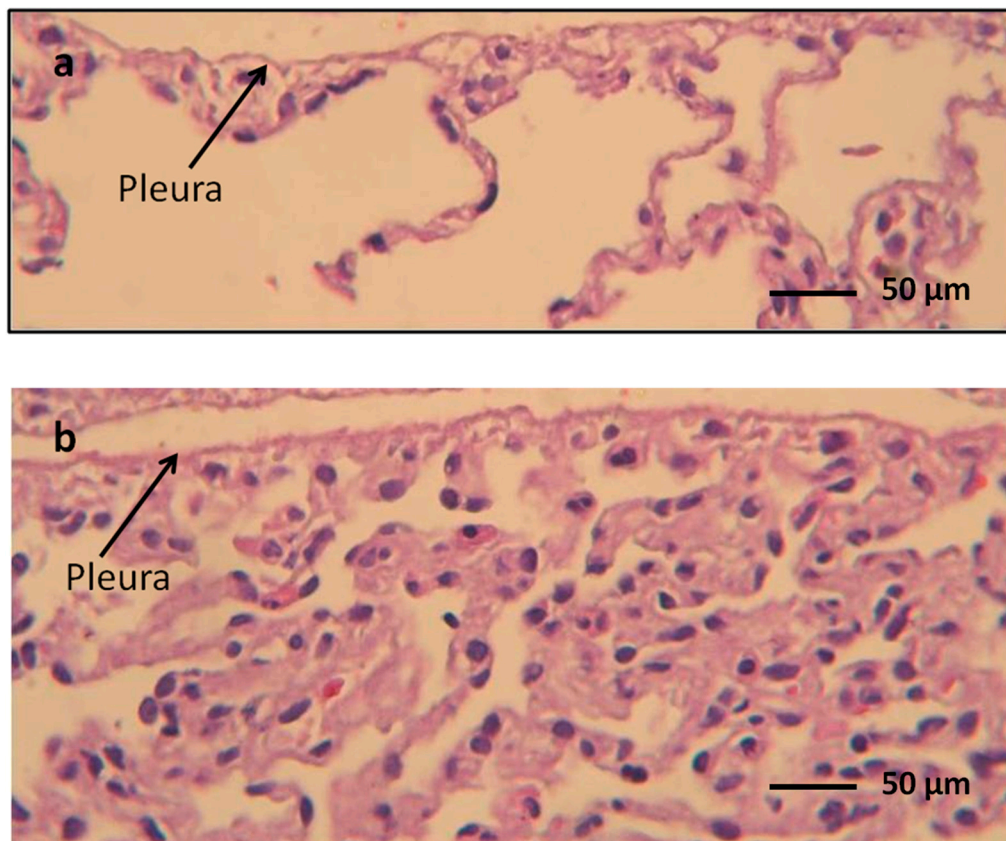


Figure 3. Histology of a normal lung (rabbit). (a) Normally expanded lung. (b) Collapsed lung. The density and the arrangement of the remaining air spaces in the two samples is very different. The subpleural limit of the parenchyma in picture B shows numerous parenchymal densities capable of trapping ultrasound, independently of the existence of interstice pathology.

For example, we can consider as cases of relatively ordered patterns of acoustic traps the early pulmonary edema and the so-called white lung. Instead examples of pathologically disordered pleura, in terms of full and empty spaces, are likely represented by idiopathic pulmonary fibrosis, Adult Respiratory Distress Syndrome (ARDS) and other pathological conditions able to subvert the sub-pleural architecture [4,28,33] (Table 1).

The distribution of air under the pleural plane in patients with early cardiogenic pulmonary edema is characterized by the presence of thickened but anatomically intact interlobular septa. In cardiogenic edema there is an expansion of the large interstitial connective tissue space caused by transudative fluid. This fluid may be confined to the large interstice and periarterial sheaths [29]. Therefore, interlobular septa enlargement can anticipate the expansion of alveolar wall interstitial space, and swollen connective tissue planes may be seen next to essentially normal alveoli.

This is not true, however, in Idiopathic Pulmonary Fibrosis, Adult Respiratory Distress Syndrome (ARDS), during parenchymal inflammation, or when the cardiogenic pulmonary edema reaches the stage of the alveolar flooding [34]. The “deterministic”, and relatively ordered, septal enlargement seen in early cardiogenic edema, which spares the lobular integrity, is lost in these conditions. The result is a more heterogeneous porosity beneath the pleural mesothelial layer in patients with ARDS, interstitial pneumonia and late stage hydrostatic pulmonary edema, in comparison with subjects with early cardiogenic edema [35] (Table 1).

Table 1. Possible relationships between Leslie’s different histopathological patterns [12,16] and the expected pulmonary ultrasound artifacts, according to the hypothesis introduced in the review.

Hystopatologic Pattern	Expected Artefacts	Examples of Pathology
Near normal lung	<p>No artefacts</p> <p>No artefact or rare artifacts from secondary hypoventilation</p> <p>No artefacts</p> <p>Bright isolated vertical artefacts, with or without internal structure, showing tendentially high native frequencies (about 6 MHz)</p> <p>Bilateral expression of artifacts without spared areas</p>	<p>Pulmonary hypertension</p> <p>Airway diseases</p> <p>Emphysema</p> <p>Air cysts</p> <p>Early and moderate cardiogenic pulmonary edema</p>
Fibrosis	<p>Irregular pleura (cobblestone), vertical merged artifacts prevalent at the lung basis, multiform artifacts in middle and lower fields, generally without internal structure, with tendentially low native frequencies (about 3 MHz).Some artifacts fade quickly.</p> <p>Many different types of vertical artifacts that are unevenly distributed in the lung areas typical of individual pathologies, irregular pleura depending on the disease</p>	<p>Idiopathic pulmonary fibrosis</p> <p>Connective tissue diseases</p> <p>Chronic hypersensitivity pneumonitis</p> <p>Chronic cardiac congestion</p> <p>Drug toxicity</p>
Acute lung injury	<p>Appearance similar to the Fibrosis pattern.</p> <p>Inhomogeneous artefactual pattern characterized by more than one native frequency, with spared areas. Possible presence of thin, brilliant and internally structured artifacts in inhomogeneous distribution.</p> <p>Relative representation of coalescent artifacts and white lung, showing inhomogeneous and variable arrangement</p>	<p>Diffuse alveolar damage</p> <p>Infections</p> <p>Acute aspiration</p> <p>Diffuse alveolar hemorrhage</p> <p>Early ARDS</p> <p>Late cardiogenic pulmonary edema (alveolar flooding)</p>
Chronic cellular infiltrates	<p>Appearance similar to Acute lung injury pattern.</p> <p>White lung and merged, thin and modulated vertical artifacts may be absent as they tend to indicate an acute phase of disease</p>	<p>Viral and fungal infections</p> <p>Hypersensitivty pneumonitis</p> <p>Atypical mycobacterial infections</p> <p>Connective tissue diseases</p> <p>Lymphangitic carcinoma</p> <p>Lymphoid interstitial pneumonia and limphoma</p> <p>Smoking related disease</p>

Table 1. *Cont.*

Hystopatologic Pattern	Expected Artefacts	Examples of Pathology
Alveolar filling	Combined aspect of vertical, variable, very heterogeneous artifacts, and subpleural consolidation. Many native frequencies	Organizing diffuse alveolar damage and infections Bacterial infections Pulmonary alveolar proteinosis Eosinophilic lung diseases Drug toxicity ARDS
Nodules	Nodules can be visible using a linear probes if located at pleural level. They acquire suggestive locations depending on the disease and often appear like vertical artifacts with nodular and non-point-like origin	Carcinomas, sarcomas, melanoma Lymphoma Lymphoid interstitial pneumonia Necrotizing infections Granulomatous infections Sarcoidosis Pneumoconiosis

The lung artifactual pattern sometimes called White Lung (Figure 4) is characterized by a granular and mostly white texture, which starts at the pleura line and ends at the bottom of the screen. Together with the pattern characterized by very homogeneous and confluent vertical artifacts, it appears to correlate with CT ground glass attenuation [36].

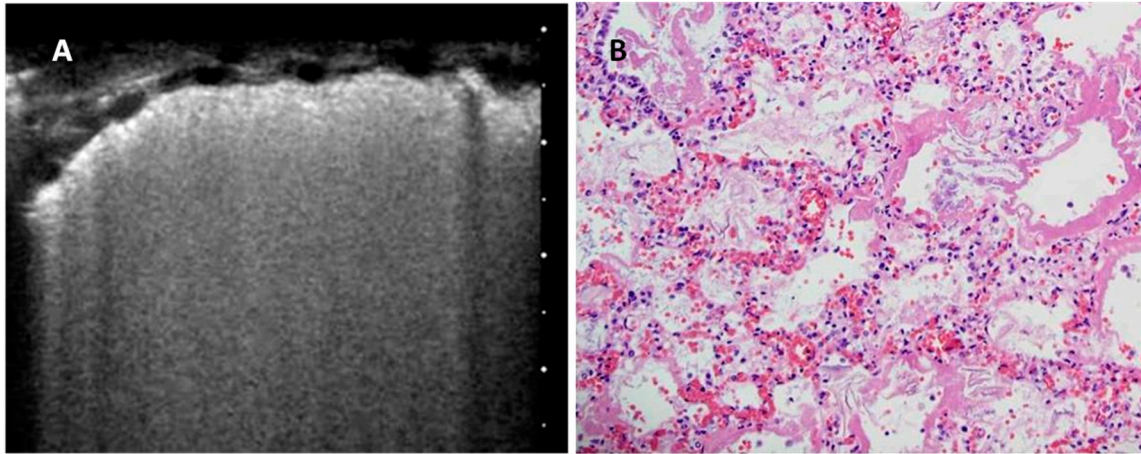


Figure 4. (A): The picture represents a pulmonary scan of a newborn with Hyaline membrane disease, showing White lung (Image obtained with a commercially available machine, Esaote MyLab 25 equipped with a linear probe 10 MHz). On the right (B) the corresponding histopathological picture. Residual airspaces are small (about 50 μm), separated by a mean distance in the order of 100–150 μm . In this condition the small diameter of the scattering bubbles and their small relative distance are probably the prerequisites for this acoustic effect.

The White Lung pattern suggests the presence of a relatively homogeneous scatterer distribution (many small airspaces close to each other which contribute to the formation of many small acoustic traps) which gives rise to numerous multiple reflections. A random distribution of small and close scattering air bubbles is needed to obtain such a pattern [33]. In this case, the expected histology is consistent with a diffuse pathological reduction of the air spaces which, however, would remain surrounded by enough interstitium to allow the type of interaction just described. In white lung, the distribution of the scatterers does not deny the existence of a relatively ordered porous structure.

Usual Interstitial Pneumonia (UIP) is the histopathologic pattern of Idiopathic Pulmonary Fibrosis (IPF) [31], characterized by “temporally heterogeneous” interstitial fibrosis and honeycombing, in which zones of normal lung tissue are adjacent to zones of advanced architectural remodeling. Fibroblastic foci occur at the interface between dense scar and adjacent normal lung. The abnormalities of IPF are most prominent at the periphery of the lungs (sub-pleural tissue, easily explored by ultrasound) and in the lung bases, regardless of the stage. Acute exacerbations [37] are expected in the history of patients with IPF and they show pathological pictures of diffuse alveolar damage or organizing pneumonia, superimposed on a background of peripherally accentuated lobular fibrosis with honeycombing. Therefore, the full/empty ratio in the sub-pleural tissue of patients with IPF is characterized by the presence of larger, irregular, attenuating acoustic traps with small residual airspaces (Figure 5). From a hystomorphometric two-dimensional point of view, the pleural plane shows a very heterogeneous and irregular distribution of “full” areas (the acoustic traps). This relative disorder can be described with the use of some algorithms, which can appreciate the 2D characteristics of the traps, such as their number, thickness, perimeter, area, and connectivity [38].

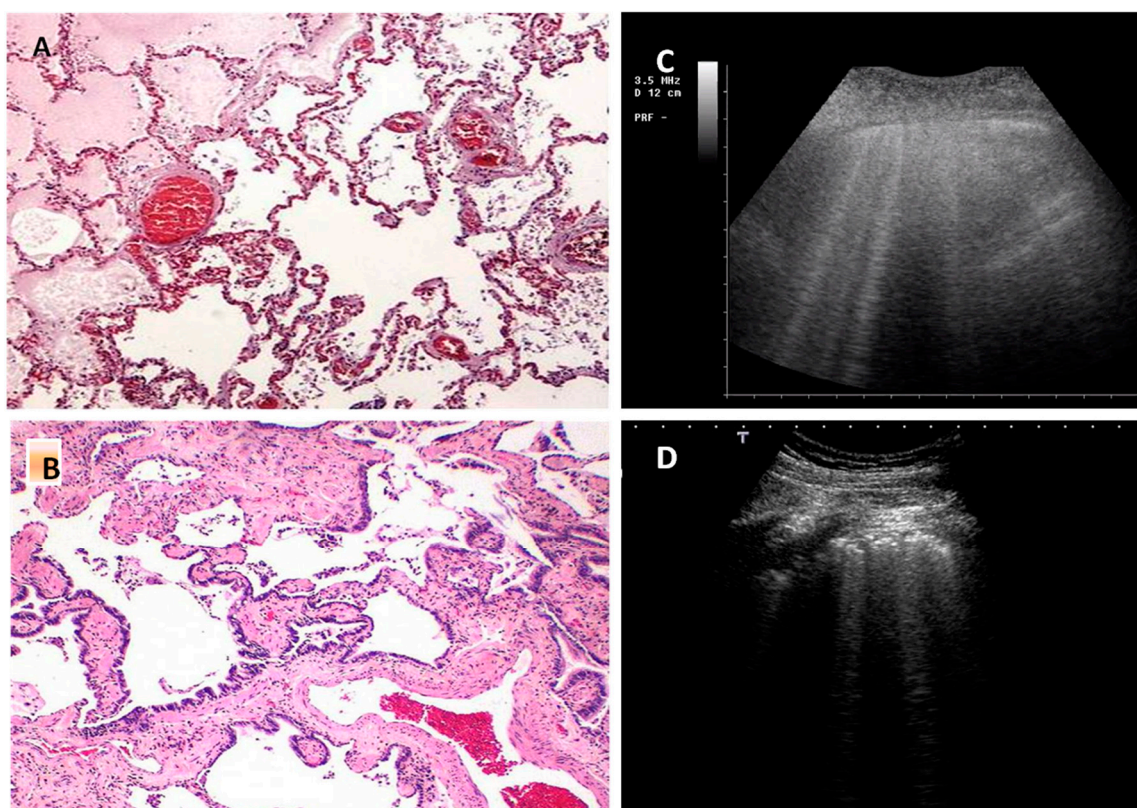


Figure 5. (A): Acute cardiogenic pulmonary edema, histopathologic picture. (B): Idiopathic Pulmonary Fibrosis (IPF), histopathologic picture. In acute pulmonary edema the lung shows little structural changes and this is especially evident in early hydrostatic edema, when only the interlobular septa show a moderate smooth thickening. On the contrary, in IPF the lung is involved by variable amount of fibrosis and it is deeply subverted in the structure. (C) and (D): The related ultrasound pictures. In cardiogenic pulmonary edema (C) pleural line is regular and smooth (Image obtained with a commercially available machine, Esaote MyLab 25 equipped with a Convex probe), in IPF (D), pleural line is irregular and the artefacts are very heterogeneous (Image obtained with a commercially available machine, Toshiba Aplio XV, equipped with a convex probe, 3 MHz, without harmonic imaging).

5. How Acoustic Traps Work

A hypothesis able to explain the genesis of vertical lung artifacts in hyperdense non consolidative pathology of the lung cortex states that the artifacts represent acoustic information relative to the full/empty ratio of the sub-pleural tissue [23,24]. Vertical artifacts are thus the visual representations of the signals originating from the multiple reflections experienced by ultrasound waves when trapped inside the channels that can form between the air spaces when a pathologic condition exists [18]. Because the acoustic trap configuration and volume, its shape and its content are variable, it is not surprising that the vertical artifacts look different in different diseases and in different stages of a single disease.

It is interesting to note that in theory every acoustic trap has its own spectral signature [39], which can be approximated accordingly to the simplified Equation [33]:

$$f_{n,m,l} = \frac{c_s}{2} \sqrt{\left(\frac{n}{d_1}\right)^2 + \left(\frac{m}{d_2}\right)^2 + \left(\frac{l}{d_3}\right)^2}$$

where $f_{n,m,l}$ represents the harmonics generated inside the acoustic trap, n , m , and l are integer numbers (harmonic components of the spectral signature of the trap), and d_1 , d_2 , and d_3 refer to the shape of the

acoustic trap (in this case simply defined by three spatial dimensions d_1 , d_2 , and d_3). Finally, C_s is the speed of sound within the trap, which is relative to the content of the trap itself.

Therefore, the determinants of the spectral signature of the traps are their content, and the dimensions and shape of their volume. For example, a spherical volume can be described by a single spatial measure, the diameter. In general, the lowest native frequency of a trap increases as the size of the trap decreases [33,39]. Obviously, the shape of a real acoustic trap, given by any transonic volume surrounded by alveoli, often cannot be described by single spatial measure. It follows that, in many cases, a more complex spectral signature is expected.

In practical terms the sequence of events producing vertical artifacts arising from a diseased pleura covering a hyperdense non-consolidated lung can be exemplified as follows: (a) the ultrasonic pulse that reach the pleura is characterized by a frequency band; (b) Such a pulse can activate specific native frequencies of the acoustic trap, in this process the access channel must allow the penetration of sufficient acoustic energy, able to generate a visible artifact on the ultrasound images; (c) The trap acts as a secondary ultrasound source and part of the trapped energy is reradiated to the probe across the entry/exit of the trap; and (d) The probe, accordingly to its transfer function, is able to capture only those signals which fall within a specific frequency range, which are then converted by pre-defined signal processing operations into vertical artifacts that assume a specific visual structure observable on the screen. The generation of an artifact may involve either only one trap at a time, as in the case of an isolated B-line, or multiple smaller acoustic traps, as in the case of the White Lung [33].

According to this view, two interesting topics for discussion come out. The first concerns the correlation between the superficial histopathology of the lung, the formation of acoustic traps, and the diagnostic information provided by the artifactual visualization of the pathological lung. The study of these artifactual phenomena is able to characterize the surface of the lung in terms of full and empty, thus giving indirect information about the morphology and structure of the peripheral pathological lung. This topic will be discussed in the following paragraph.

The second topic concerns the instrumentation suitable for capturing the acoustic information contained in the artifacts. As largely discussed in a recent technical review [40] and briefly introduced in this paper, standard pulse-echo ultrasound imaging is clearly not designed for lung tissue. In fact, commercial ultrasound systems are finely tuned to detect and image only small acoustic impedance mismatches, and this assumption is not verified in the case of the lung. To date, the acoustic information contained in the individual and visually variable vertical artifacts can be lost or difficult to interpret, because their evaluation is subjective and it is not based on the knowledge of their physical origin [41]. Research effort should thus focus on the development of an ultrasound method dedicated to the peculiarities of lung tissue.

6. Future Perspectives

Sonographic diagnosis of pulmonary edema and ARDS is well known and appreciated in Emergency Medicine and Critical Care settings. The use of lung ultrasound is less common among pulmonologists for the study of interstitial pulmonary disease [42,43]. In 2008, some criteria for ultrasound differential diagnosis between ARDS and Cardiogenic Pulmonary Edema (CPE) were proposed [35]. The differences concerned the regularity of the pleural line in CPE and the distribution of the artifacts, more regular in CPE and showing a patchy aspect with spared areas in ARDS. In 2017, these criteria were reviewed [36], paying particular attention to the morphology of the individual artifacts and hypothesizing a correlation between their appearance and the sub-pleural histology, obviously different in the two pathologic conditions. Moreover, there is no doubt that independently of the pulmonary density, the ultrasound picture of the lung in CPE is very different (Figure 5) from that of primitive and secondary pulmonary interstitial disease [36,44]. These observations support the hypothesis that the superficial histopathology of the lung responds to ultrasound through the creation of different acoustic traps in the different pathologies, which are capable of conditioning the appearance of the vertical artifact and their distribution along the pleural surface.

A characteristic of the vertical artifacts that appear in pulmonary ultrasound, which has recently been confirmed in the literature [4,33], is the internal structure of the single artifact (Figure 2). Every artifact has its own structure. It can be seen as a sequence of alternating white and black horizontal bands, or appear as a sequence of bands with two similar gray levels, or showing a constant white or gray level. A possible physical explanation of these variability was recently described in an article [33], but, in general terms, the artifactual pattern changes from White Lung to multiple unstructured vertical artifacts and, subsequently, to isolated modulated or non-modulated vertical artifacts by progressively increasing the dominance of the air spaces. Whereas the internal structure of the vertical artifacts is related to the size of the traps, their regularity, and to the transmitted frequency band and the transfer function of the probe.

If we will be able to translate these considerations into practice, ultrasonography of the still aerated pathological lung would represent a surface tissue characterization in which the density of the tissue is expressed by the concentration of artifacts (from rare artifacts to the white lung). The appearances of the individual artifacts (determined by their native frequencies [39]) could instead express the physical characteristics of the acoustic traps related to the underlying histopathology. Finally, a relatively orderly histopathology (initial cardiogenic edema, initial acute lung injury) could show a higher degree of morphological uniformity of the vertical artifacts compared to diseases that profoundly subvert the structure of the lung such as fibrosis.

This means, on the one hand that the native frequency of the vertical artefacts in pulmonary ultrasound may be used to quantitatively characterize the physical properties of the sub-pleural lung, and on the other hand, that the development of an ultrasound method that is specific and dedicated to the lung is certainly timely and desirable.

One final remark should also be made about safety. Diagnostic ultrasound has been widely used in clinical medicine for long time with no proven deleterious effect. Lung exposition to ultrasound is obvious during breast ultrasound, echocardiography and chest sonography without any practical effect clinically documented. However, high levels of acoustic energy can produce temperature raises that are hazardous to the embryo and fetus and sensitive organs (investigation of the eye, neonatal echocardiography, and cranial investigation of the new-born).

Moreover, diagnostic ultrasound has been proven not to be completely harmless on lung tissue in mice. Evidence of pulmonary hemorrhage has been reported as function of frequency and mechanical index [45,46], although there was no clear tendency for thresholds to increase with increasing ultrasonic frequency when pulse-timing conditions were similar [47].

Consequently, users of chest ultrasound should check both the thermal and the mechanical index of the machine, keeping them as low as reasonably achievable without compromising the value of the examination. Finally, diagnostic ultrasound methods dedicated to the lung should not be characterized by long exposure time [48].

Author Contributions: Conceptualization, G.S.; Technical support, L.D.; Writing—original draft preparation, G.S., A.S., L.D. and R.I.; review and editing, G.S., A.S., L.D. and R.I. All authors have read and agreed to the published version of the manuscript.

Funding: This research received no external funding.

Conflicts of Interest: The authors declare no conflict of interest.

References

1. Volpicelli, G.; Elbarbary, M.; Blaivas, M.; Lichtenstein, D.A.; Mathis, G.; Kirkpatrick, A.W.; Melniker, L.; Gargani, L.; Noble, V.E.; Via, G.; et al. International Liaison Committee on Lung Ultrasound (ILC-LUS) for the International Consensus Conference on Lung Ultrasound (ICC-LUS). International evidence-based recommendations for point-of-care lung ultrasound. *Intensive Care Med.* **2012**, *38*, 577–591. [[CrossRef](#)]
2. Sekiguchi, H.; Schenck, L.A.; Horie, R.; Suzuki, J.; Lee, E.H.; McMenemy, B.P. Critical care ultrasonography differentiates ARDS, pulmonary edema, and other causes in the early course of acute hypoxemic respiratory failure. *Chest* **2015**, *148*, 912–918. [[CrossRef](#)] [[PubMed](#)]

3. Vignon, P.; Repessè, X.; Vieillard Baron, A.; Maury, E. Critical care ultrasonography in acute respiratory failure. *Crit. Care* **2016**, *20*, 228. [[CrossRef](#)] [[PubMed](#)]
4. Soldati, G.; Demi, M.; Smargiassi, A.; Inchingolo, R.; Demi, L. The role of ultrasound lung artifacts in the diagnosis of respiratory diseases. *Expert Rev. Respir. Med.* **2019**, *13*, 163–172. [[CrossRef](#)] [[PubMed](#)]
5. Koegelenberg, C.F.; von Groote-Bidlingmaier, F.; Bolliger, C.T. Transthoracic ultrasonography for the respiratory physician. *Respiration* **2012**, *84*, 337–350. [[CrossRef](#)]
6. Mayo, P.H.; Copetti, R.; Feller-Kopman, D.; Mathis, G.; Maury, E.; Mongodi, S.; Mojoli, F.; Volpicelli, G.; Zanobetti, M. Thoracic ultrasonography: A narrative review. *Intensive Care Med.* **2019**, *45*, 1200–1211. [[CrossRef](#)]
7. Reissig, A.; Copetti, R.; Mathis, G.; Mempel, C.; Schuler, A.; Zechner, P.; Aliberti, S.; Neumann, R.; Kroegel, C.; Hoyer, H. Lung ultrasound in the diagnosis and follow-up of community-acquired pneumonia: A prospective, multicenter, diagnostic accuracy study. *Chest* **2012**, *142*, 965–972. [[CrossRef](#)]
8. Lichtenstein, D.; Goldstein, I.; Mourgeon, E.; Cluzel, P.; Grenier, P.; Rouby, J.J. Comparative diagnostic performances of auscultation, chest radiography, and lung ultrasonography in acute respiratory distress syndrome. *Anesthesiology* **2004**, *100*, 9–15. [[CrossRef](#)]
9. Brogi, E.; Bignami, E.; Sidoti, A.; Shawar, M.; Gargani, L.; Vetrugno, L.; Volpicelli, G.; Forfori, F. Could the use of bedside lung ultrasound reduce the number of chest x-rays in the intensive care unit? *Cardiovasc. Ultrasound* **2017**, *13*, 23. [[CrossRef](#)]
10. Smargiassi, A.; Inchingolo, R.; Chiappetta, M.; Ciavarella, L.P.; Lopatriello, S.; Corbo, G.M.; Margaritora, S.; Richeldi, L. Agreement between chest ultrasonography and chest X-ray in patients who have undergone thoracic surgery: Preliminary results. *Multidiscip. Respir. Med.* **2019**, *4*, 9. [[CrossRef](#)]
11. Agricola, E.; Arbelot, C.; Blaivas, M.; Bouhemad, B.; Copetti, R.; Dean, A.; Dulchavsky, S.; Elbarbary, M.; Gargani, L.; Hoppmann, R.; et al. Ultrasound performs better than radiographs. *Thorax* **2011**, *66*, 828–829. [[CrossRef](#)] [[PubMed](#)]
12. Reissig, A.; Kroegel, C. Sonographic diagnosis and follow-up of pneumonia: A prospective study. *Respiration* **2007**, *74*, 537–547. [[CrossRef](#)] [[PubMed](#)]
13. Lichtenstein, D.; Mezière, G.; Seitz, J. The dynamic air bronchogram. A lung ultrasound sign of alveolar consolidation ruling out atelectasis. *Chest* **2009**, *135*, 1421–1425. [[CrossRef](#)] [[PubMed](#)]
14. Sartori, S.; Postorivo, S.; Vece, F.D.; Ermili, F.; Tassinari, D.; Tombesi, P. Contrast-enhanced ultrasonography in peripheral lung consolidations: What's its actual role? *World J. Radiol.* **2013**, *28*, 372–380. [[CrossRef](#)]
15. Soni, N.J.; Franco, R.; Velez, M.I.; Schnobrich, D.; Dancel, R.; Restrepo, M.I.; Mayo, P.H. Ultrasound in the diagnosis and management of pleural effusions. *J. Hosp. Med.* **2015**, *10*, 811–816. [[CrossRef](#)]
16. Smargiassi, A.; Pasciuto, G.; Pedicelli, I.; Lo Greco, E.; Calvello, M.; Inchingolo, R.; Schifino, G.; Capoluongo, P.; Patriciello, P.; Manno, M.; et al. Chest ultrasonography in health surveillance of asbestos-related lung diseases. *Toxicol. Ind. Health* **2017**, *33*, 537–546. [[CrossRef](#)]
17. Smargiassi, A.; Inchingolo, R.; Zanforlin, A.; Valente, S.; Soldati, G.; Corbo, G.M. Description of free-flowing pleural effusions in medical reports after echographic assessment. *Respiration* **2013**, *85*, 439–441. [[CrossRef](#)]
18. Lichtenstein, D.; Mezière, G.; Biderman, P.; Gepner, A.; Barrè, O. The comet-tail artifact: An ultrasound sign of alveolar interstitial syndrome. *Am. J. Respir. Crit. Care Med.* **1997**, *156*, 1640–1646. [[CrossRef](#)]
19. Dietrich, C.F.; Mathis, G.; Blaivas, M.; Volpicelli, G.; Seibel, A.; Wastl, D. Lung B-line artefacts and their use. *J. Thorac. Dis.* **2016**, *8*, 1356–1365. [[CrossRef](#)]
20. Reissig, A.; Copetti, R.; Kroegel, C. Current role of emergency ultrasound of the chest. *Crit. Care Med.* **2011**, *39*, 839–845. [[CrossRef](#)]
21. Dulchavsky, S.A.; Schwarz, K.L.; Kirkpatrick, A.W.; Billica, R.D.; Williams, D.R.; Diebel, L.N.; Campbell, M.R.; Sargysan, A.E.; Hamilton, D.R. Prospective evaluation of thoracic ultrasound in the detection of pneumothorax. *J. Trauma* **2001**, *50*, 201–205. [[CrossRef](#)] [[PubMed](#)]
22. Lichtenstein, D.A.; Mezière, G.A. Relevance of lung ultrasound in the diagnosis of acute respiratory failure: The BLUE protocol. *Chest* **2008**, *134*, 117–125. [[CrossRef](#)] [[PubMed](#)]
23. Smargiassi, A.; Inchingolo, R.; Soldati, G.; Copetti, R.; Marchetti, G.; Zanforlin, A. The role of chest ultrasonography in the management of respiratory diseases: Document II. *Multidiscip. Respir. Med.* **2013**, *8*, 55. [[CrossRef](#)] [[PubMed](#)]
24. Soldati, G.; Smargiassi, A.; Inchingolo, R.; Sher, S.; Nenna, R.; Valente, S. Lung ultrasonography may provide an indirect estimation of lung porosity and airspace geometry. *Respiration* **2014**, *88*, 458–468. [[CrossRef](#)]

25. Soldati, G.; Inchingolo, R.; Smargiassi, A.; Sher, S.; Nenna, R.; Inchingolo, C.D.; Valente, S. Ex vivo lung sonography: Morphologic-ultrasound relationship. *Ultrasound Med. Biol.* **2012**, *38*, 1169–1179. [[CrossRef](#)]
26. Beckh, S.; Bolcskei, P.L.; Lessnau, K.D. Real time chest ultrasonography: A comprehensive review for the pulmonologist. *Chest* **2000**, *122*, 1759–1773. [[CrossRef](#)]
27. Leslie, K.; Wick, M. *Practical Pulmonary Pathology. A Diagnostic Approach*, 1st ed.; Churchill-Livingstone: Philadelphia, PA, USA, 2005.
28. Soldati, G.; Demi, M.; Inchingolo, R.; Smargiassi, A.; Demi, L. On the Physical Basis of Pulmonary Sonographic Interstitial Syndrome. *J. Ultrasound Med.* **2016**, *35*, 2075–2086. [[CrossRef](#)]
29. Slavin, G.; Kreel, L.; Herbert, A.; Sandin, B. Pulmonary oedema at necropsy: A combined pathological and radiological method of study. *J. Clin. Pathol.* **1975**, *28*, 357–366. [[CrossRef](#)]
30. Raghu, G.; Remy-Jardin, M.; Myers, J.L.; Richeldi, L.; Ryerson, C.J.; Lederer, D.J. Diagnosis of Idiopathic Pulmonary Fibrosis. An official, ATS/ERS/JRS/ALAT Clinical Practice Guideline. *Am. J. Respir. Crit. Care Med.* **2018**, *198*, 44–68. [[CrossRef](#)]
31. Leslie, K.O. Pathology of interstitial lung disease. *Clin. Chest Med.* **2004**, *25*, 657–703. [[CrossRef](#)]
32. Leslie, K.O. My approach to interstitial lung disease using clinical, radiological and histopathological patterns. *J. Clin. Pathol.* **2019**, *62*, 387–401. [[CrossRef](#)] [[PubMed](#)]
33. Demi, M.; Prediletto, R.; Soldati, G.; Demi, L. Physical mechanisms providing clinical informations from ultrasound lung images: Hypothesis and early confirmations. *IEEE Trans. Ultrason. Ferroelectr. Freq. Control* **2019**. [[CrossRef](#)] [[PubMed](#)]
34. Milne, E.N.; Pistolesi, M.; Miniati, M.; Giuntini, C. The radiologic distinction of cardiogenic and non cardiogenic edema. *AJR* **1985**, *144*, 879–894. [[CrossRef](#)] [[PubMed](#)]
35. Copetti, R.; Soldati, G.; Copetti, P. Chest sonography: A useful tool to differentiate acute cardiogenic pulmonary edema from Acute respiratory distress syndrome. *Cardiovasc. Ultrasound* **2008**, *6*, 16. [[CrossRef](#)]
36. Soldati, G.; Demi, M. The use of lung ultrasound images for the differential diagnosis of pulmonary and cardiac interstitial pathology. *J. Ultrasound* **2017**, *20*, 91–96. [[CrossRef](#)]
37. Kolb, M.; Bondue, B.; Pesci, A.; Miyazaki, Y.; Song, J.W.; Bhatt, N.Y. Acute exacerbations of progressive-fibrosing interstitial lung diseases. *Eur. Respir. Rev.* **2018**, *27*. [[CrossRef](#)]
38. Dalle Carbonare, L.; Valenti, M.T.; Bertoldo, F.; Zanatta, M.; Zenari, S.; Realdi, G. Bone microarchitecture evaluated by histomorphometry. *Micron* **2005**, *36*, 609–616. [[CrossRef](#)]
39. Demi, L.; van Hove, W.; van Sloun, R.J.G.; Soldati, G.; Demi, M. Determination of a potential quantitative measure of the state of the lung using lung ultrasound spectroscopy. *Sci. Rep.* **2017**, *7*, 12746. [[CrossRef](#)]
40. Demi, L.; Egan, T.; Muller, M. Lung ultrasound imaging, a technical review. *Appl. Sci.* **2020**, *10*, 462. [[CrossRef](#)]
41. Demi, L.; Demi, M.; Smargiassi, A.; Inchingolo, R.; Faita, F.; Soldati, G. Ultrasonography in lung pathologies: New perspectives. *Multidiscip. Respir. Med.* **2014**, *9*, 27. [[CrossRef](#)]
42. Reissig, A.; Kroegel, C. Transthoracic sonography of diffuse parenchymal lung disease: The role of comet tail artifacts. *J. Ultrasound Med.* **2003**, *22*, 173–180. [[CrossRef](#)] [[PubMed](#)]
43. Hasan, A.A.; Makhlof, H.A. B-lines: Transthoracic chest ultrasound signs useful in assessment of interstitial lung diseases. *Ann. Thorac. Med.* **2014**, *9*, 99–103.
44. Singh, A.K.; Mayo, P.H.; Koenig, S.; Talwar, A.; Narasimhan, M. The Use of M-Mode Ultrasonography to Differentiate the Causes of B Lines. *Chest* **2018**, *153*, 689–696. [[CrossRef](#)] [[PubMed](#)]
45. Child, S.Z.; Hartman, C.L.; Schery, L.A.; Carstensen, E.L. Lung damage from exposure to pulsed ultrasound. *Ultrasound Med. Biol.* **1990**, *16*, 817–825. [[CrossRef](#)]
46. Miller, D.L. Induction of pulmonary hemorrhage in rats during diagnostic ultrasound. *Ultrasound Med. Biol.* **2012**, *38*, 476–482. [[CrossRef](#)] [[PubMed](#)]
47. Miller, D.L.; Dou, C.; Raghavendran, K. Pulmonary Capillary Hemorrhage Induced by Fixed-Beam Pulsed Ultrasound. *Ultrasound Med. Biol.* **2015**, *41*, 2212–2219. [[CrossRef](#)] [[PubMed](#)]
48. Haar, G. Ultrasonic imaging: Safety considerations. *Interface Focus* **2011**, *1*, 686–697. [[CrossRef](#)]

